Carbon K-shell near-edge structure calculations for graphite using the multiple-scattering approach

1996 J. Phys.: Condens. Matter 8 3835

(http://iopscience.iop.org/0953-8984/8/21/010)

J. Phys.: Condens. Matter **8** (1996) 3835–3841. Printed in the UK

Carbon K-shell near-edge structure calculations for graphite using the multiple-scattering approach

D G McCulloch† and R Brydson‡

† Electron Microscope Unit and Australian Key Centre for Microscopy and Microanalysis, University of Sydney, NSW 2006, Australia

‡ School of Materials, University of Leeds, Leeds, West Yorkshire LS2 9JT, UK

Received 17 November 1995, in final form 27 February 1996

Abstract. The near-edge absorption fine structure of carbon in graphite has been calculated using the multiple-scattering approach. The effects of both a neutral carbon absorber and taking into account the effect of the core hole by using a nitrogen ($Z+1$) absorber atom are considered. The best agreement with experiment was obtained for the case of the nitrogen absorber and a cluster of 145 atoms, with the calculated near-edge structure (NES) containing the main features observed experimentally. A splitting near the onset of the σ^*-peak, similar to that seen experimentally, was found to occur in the calculated NES for one of the two inequivalent carbon atoms in the graphite structure. This splitting was not observed in the calculated NES for a single sheet of graphite, supporting the proposition that it only occurs in well ordered graphite. This result supports the proposition that the splitting originates from a sharp σ^*-peak and a dipole-allowed bandlike contribution associated to the Γ_2^- branch of the free-electron-like interlayer states.

1. Introduction

The ability of x-ray absorption spectroscopy (XAS) and electron energy-loss spectroscopy (EELS) to accurately determine chemical compositions from inner-shell loss edges is well known. In addition to elemental concentrations, each characteristic absorption edge exhibits structure which provides information on the atomic environment of the absorbing atom [1, 2]. The strong oscillations which occur within about 40 eV of the Fermi energy are known as near-edge structure (NES). NES reflects the local density of unoccupied states and is therefore strongly dependent on the local atomic environment. Extended fine structure involves the study of the weaker oscillations superimposed on the core loss edge extending from about 40 eV from the Fermi energy. By applying a single-scattering theory, these oscillations can be used to determine the radial distribution function [1]. The lower kinetic energy of the ejected electron in NES means that multiple-scattering effects are strong, and more detailed structural information on multi-atom correlations, such as the spatial arrangement of the atoms neighbouring the absorbing one, can be obtained.

Multiple-scattering (MS) theory is an approach to calculating NES which can be considered as an extension of the extended fine-structure single-scattering theory by considering all possible scattering paths for the ejected electron within a cluster of atoms [2]. MS is more flexible than band-structure calculations for determining NES because this real-space approach provides advantages in interpreting features in the NES and allows the calculation of NES for more complex structures. In the present work, MS theory has been

0953-8984/96/213835+07$19.50

employed to calculate the NES of graphite. On considering larger cluster sizes and the effect of the core hole, the calculated NES more closely matches experimental observations than do previous MS calculations [2, 3]. In addition, by studying the effect of increasing cluster size on the NES, features which are observed in the NES of graphite can be related to the effect of certain atoms in the graphite cluster.

2. Theory

The MS approach for calculating NES is based on the interference between the electron wave generated by the ejection of an inner-shell electron and the electron wave backscattered from surrounding atoms [1, 2]. In quantum mechanical terms, this interference modifies the final-state wave functions available to the ejected electron. Although MS was developed for the study of x-ray absorption near-edge structure (XANES), it is applicable to electron energy-loss near-edge structure (ELNES) for small collection angles where the momentum transfer is small and dipole transitions dominate. In MS, the scattering properties of each type of atom, expressed in the form of phase shifts for incident spherical waves of angular momentum l, are calculated assuming muffin-tin potentials obtained by the Mattheiss prescription [4]. The NES for the cluster of atoms is then calculated by multiplying the resultant interference by the square of the atomic transition matrix for the absorbing atom. The computer program used was that of Vvedensky, Saldin and Pendry (see [5, 6]), where the cluster is divided into shells of atoms approximately equidistant from the absorbing atom. The MS within each shell is calculated and then scattering between shells is determined; combining the two determines the MS for the cluster. This method allows the effect on the near-edge structure of various cluster sizes to be determined, enabling the association of various features in the NES to be identified with particular scatterers within the cluster.

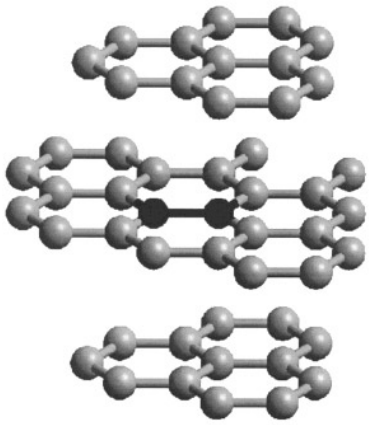

Figure 1. The crystal structure of graphite showing the two inequivalent carbon atoms (shown in black) which have either two or twelve c-axis nearest neighbours.

As indicated in figure 1, there are two inequivalent carbon atoms within the graphite structure. These can be classified by the number of interplanar or c-axis nearest neighbours that they have—either 2 or 12. Owing to the localized nature of the excitation process, in order to calculate the total NES for graphite, calculations need to be performed for both inequivalent atoms and averaged. The muffin-tin potentials were constructed using wave functions generated by the Herman–Skillman program [7], with a radius chosen to be half the nearest-neighbour distance (0.071 nm) and a statistical exchange potential (α) of 0.8 [8]. Variation of the exchange potential was found to have little effect on the resulting

ELNES. The inelastic attenuation parameter in the MS calculation, which is used as a measure of the experimental broadening, was taken to be $V_i = -0.5$ eV. Similar spectra with broadened features were calculated with $V_i = -1$ eV. In addition to a neutral atom absorber ($1s^2 2s^2 2p^2$), calculations were performed using a neutral nitrogen atom ($1s^2 2s^2 2p^3$) at the absorption site. The use of a nitrogen atom instead of a carbon atom at the absorption site is known as the $Z + 1$ potential approximation which attempts to take into account the effect of the core hole [9].

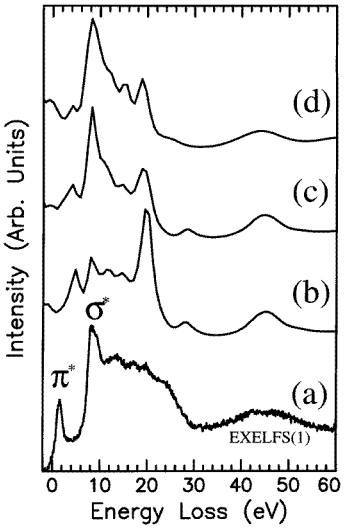

Figure 2. The carbon K edge of (a) graphite measured experimentally, and calculated using multiple scattering for (b) graphite with a neutral carbon absorber ($1s^2 2s^2 2p^2$), (c) graphite with a neutral nitrogen ($Z+1$) absorber ($1s^2 2s^2 2p^3$), and (d) a single layer of graphite with a neutral nitrogen ($Z + 1$) absorber ($1s^2 2s^2 2p^3$).

3. Experiment

For the purposes of comparison, an experimentally obtained electron energy-loss (EEL) spectrum was collected from a thin specimen of highly oriented pyrolytic graphite (HOPG) oriented with its *c*-axis nearly parallel to the electron beam. The spectrum was collected using a Gatan 666 parallel EEL spectrometer attached to a VG Microscopes HB601 scanning transmission electron microscope operating at 100 keV. The electron probe convergence semi-angle on the specimen of 13.7 mrad and a spectrometer acceptance semi-angle of 8.3 mrad were used. The energy resolution of the spectrometer, as measured by the full width at half-maximum (FWHM) of the zero-loss peak, was 0.6 eV.

4. Results and discussion

Figure 2(a) shows the experimentally obtained carbon K edge from HOPG. Since this spectrum was collected from a thin specimen of HOPG, multiple-scattering effects are small and therefore it was not necessary to deconvolute this spectrum. The spectrum has been plotted against energy loss relative to the Fermi level, taken to be 284 eV [10]. The spectrum

shown in figure 2 is in agreement with previous measurements [11]. The main features in the graphite spectrum are the 1s-to-π^* peak at about 1.5 eV, a broad peak between 8 and 25 eV which has been attributed mainly to 1s-to-σ^* transitions, and a peak at about 45 eV which corresponds to a strong oscillation in the extended fine structure (EXELFS). The sharp peak at 8.2 eV near the onset of the σ^*-peak has recently been shown to consist of two peaks when collected at high energy resolution [11]. This splitting has been attributed to two contributions: (i) a very sharp σ^*-peak at 291.65 eV; and (ii) a bandlike contribution having an onset at 291.9 eV. It was suggested that this latter peak may be due to the Γ_2^- branch of the free-electron-like interlayer states [11].

Table 1. Summary of the main peak positions in graphite determined experimentally and calculated using both a neutral carbon absorber and a neutral nitrogen absorber.

		MS calculation	
Peak	Experiment (eV)	C absorber (eV)	N absorber (eV)
1s to π^*	1.5	4.9	3.7
1s to σ^*	8.2	8.0	8.2
EXELFS (1)	45.2	44.9	44.8

Figure 2 also shows the MS calculations for graphite with (i) a neutral carbon ($1s^2 2s^2 2p^2$) absorber potential (figure 2(b)) and (ii) a nitrogen ($1s^2 2s^2 2p^3$) absorber potential ($Z + 1$) (figure 2(c)). Both spectra were the linear superpositions of the two inequivalent atom positions in the graphite structure and employed cluster sizes of 145 atoms (16 or 20 shells). Increasing the cluster size beyond this was found to have little effect on the resulting spectra. The energy scale has been shifted down in energy using an estimate for the muffin-tin zero of energy calculated in the Mattheiss muffin-tin code (about 10 eV). Table 1 summarizes the main peak positions for the graphite experimental spectrum as well as both of the neutral carbon and $(Z + 1)$ nitrogen absorber calculations. Both calculations predict the three main features present in the experimental spectrum; that is the π^*-, broad σ^*- and EXELFS peaks. However, in both calculations it is clear that the π^*-peak has a much reduced intensity and a higher than expected position relative to the experimental spectrum. The main difference between the two calculations is the difference in fine structure contained in the broad σ^*-peak. The inclusion of the core-hole approximation shifts intensity in the σ^*-peak to lower energies, closer to the onset of the conduction band. Therefore, the presence of the core hole (nitrogen absorber) provides a better overall agreement with experiment by correctly predicting the sharp peak at 8.2 eV near the onset of the broad σ^*-peak. In addition, the main peak positions listed in table 1 are closer to the experimental values for the $(Z + 1)$ absorber.

The reduced intensity and higher than expected position for the π^*-peak in both calculations can be explained by the muffin-tin approximation employed which assumes spherical potentials for each atom in the structure. Clearly in graphite this approximation is rather poor especially in the c-axis direction where the π-orbitals are located. It is well known that the muffin-tin approximation works well for close-packed structures and poorly for more dispersed structures. Therefore in graphite, it is expected that the muffin-tin approximation will lead to a poorer representation of features resulting from transitions in the interplanar direction than those resulting from transitions in the close-packed in-plane directions.

The calculated spectra shown in figure 2 appear to be closer to experiment than those

previously published by Weng, Rez and Ma [3] and Vvedensky [2], possibly due to the smaller cluster sizes used in both of those works. In addition, neither of these calculations considered core-hole effects. However, the spectra calculated in this study do not agree as well with experiment as the partial DOS calculated using a self-consistent pseudo-atomic-orbital (PAO) band-structure calculation [3]. This calculation correctly predicts the relative intensity and position of the π^*-peak as the non-spherical potentials of the carbon atoms are better represented by using pseudopotentials than they are for spherical muffin-tin potentials. However, the shape and relative intensity of the features in the σ^*-peak in the PAO band-structure calculation closely match the shape of the σ^*-peak calculated in the present study using the $(Z + 1)$ absorber. This comparison further supports the notion that the spherical muffin-tin potentials work well for the close-packed in-plane transitions in graphite while breaking down in the *c*-axis direction.

Figure 2(d) includes a MS calculation for a single layer of graphite consisting of 10 shells of atoms and a nitrogen absorber (figure 2(d)). Structures which contain good in-plane graphitic order and no correlations between planes are known as turbostratic and can be approximated by a single layer of graphite. Glassy carbon is an example of a turbostratic graphite, and has a NES similar to that seen in crystalline graphite [12]. The calculated NES for the single graphite layer is similar to the calculation for the full graphite structure confirming that the NES in graphite is dominated by in-plane correlations.

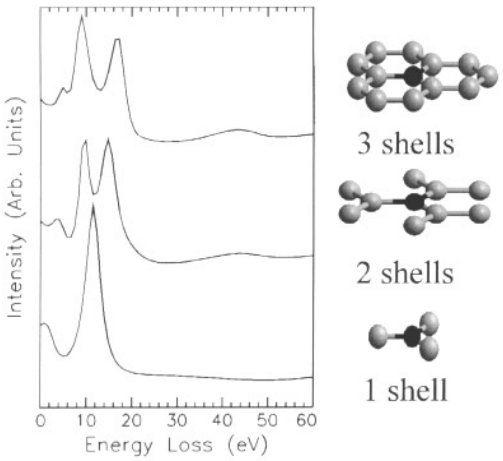

Figure 3. The carbon K edge of graphite for 1–3 shells calculated using multiple scattering with a neutral nitrogen $(Z + 1)$ absorber $(1s^2 2s^2 2p^3)$.

In order to explore the effect of increasing cluster size on the near-edge structure of graphite, MS calculations for the two inequivalent carbon atoms in the graphite structure were calculated for various cluster sizes with the cole-hole approximation included. Figure 3 shows the structure and resulting NES for the first three in-plane nearest neighbours, which are identical for both inequivalent atoms. It is apparent in this figure that the basic shape of the σ^*-peak (which consists of a peak at about 8 eV and a smaller peak at about 18 eV) is well developed after the first three shells which contain in-plane neighbouring atoms. For cluster sizes containing four or more nearest neighbours, each inequivalent atom has a different structural arrangement and the resulting NES differs as shown in figure 4. Generally the π^*-peak is more pronounced for the case where the absorber atom has twelve rather

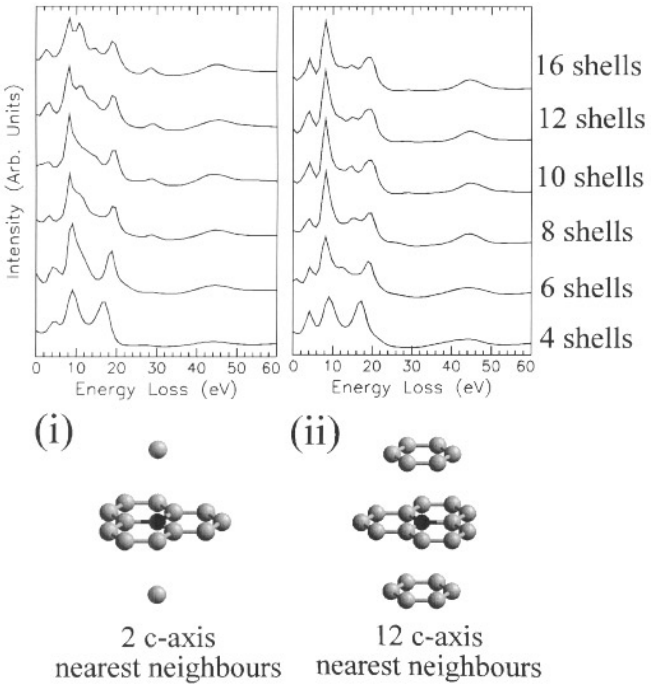

Figure 4. The effect of increasing number of shells on the calculated carbon K edge of graphite for each of the two inequivalent carbon atoms—either two or twelve.

than two *c*-axis nearest neighbours.

As the cluster size increases above four, differences in the features contained in the σ^*-peak become apparent. The most noticeable of these is a splitting in the sharp feature at about 8.2 eV near the onset of the σ^*-peak. As discussed above, a splitting in this feature has been observed in spectra collected at high energy resolution and has been attributed to a very sharp σ^*-peak at 291.65 eV in addition to a dipole-allowed bandlike contribution having an onset at 291.9 eV associated to the Γ_2^- branch of the free-electron-like interlayer states [11]. This leads to a splitting of this peak by about 1.2 eV in the energy-loss spectrum. Recent single-particle band-structure calculations have also predicted splitting in the σ^*-peak of graphite [13]. Although the splitting shown in figure 4 is greater (about 2.5 eV), it appears from the present results that the splitting originates from one of the inequivalent atoms in the graphite structure (the case of two collinear *c*-axis neighbours). In the calculations, the magnitude of this splitting appears to be sensitive to the interlayer spacing suggesting that this feature is indeed a bandlike contribution arising from σ-overlap of p_z orbitals associated with the linear chain of carbon atoms running along the *c*-axis at this site. The larger splitting of 2.5 eV rather than the 1.2 eV observed experimentally may be explained by the poor performance of the muffin-tin potentials for interplane transitions. Since the splitting only occurs for one of the inequivalent atoms, it is expected to be observed only in highly oriented graphite such as HOPG where good registry between the basal planes exists. No evidence of this splitting was seen in the calculation for a single layer of graphite. This may explain why splitting was not observed in recent synchrotron x-ray absorption fine-structure experiments on polycrystalline graphite [14] where poorer *c*-axis registry would wash out this splitting effect.

5. Conclusion

The carbon K edge in graphite has been calculated using the multiple-scattering approach with various cluster sizes and both neutral carbon and neutral nitrogen $(Z + 1)$ absorber atoms. It was found that good agreement with experiment was obtained for a cluster of 150 atoms and with a nitrogen absorber atom in order to take into account the effects due to the core hole. A splitting near the onset of the σ^*-peak was found to occur for one of the two inequivalent atoms in the graphite structure and was not observed in the calculation from a single sheet of graphite. These results are consistent with the proposition that the splitting originates from a very sharp σ^*-peak in addition to a dipole-allowed bandlike contribution associated to the Γ_2^- branch of the free-electron-like interlayer states.

Acknowledgments

This work was supported by a grant from the Australian Research Council. One of us (DGM) gratefully acknowledges the support provided by an Australian Postdoctoral Research Fellowship.

References

[1] Bianconi A 1988 *X-ray absorption Principles, Applications and Techniques of EXAFS, SEXAFS and XANES* ed D C Komomgsberger and R Prins (New York: Wiley) ch 11, p 573
[2] Vvedensky D D 1992 *Unoccupied Electronic States (Springer Topics in Applied Physics 69)* ed F J Fuggle and J E Inglesfield (Berlin: Springer) ch 5, p 139
[3] Weng X, Rez P and Ma H 1989 *Phys. Rev.* B **40** 4175
[4] Mattheiss L F 1964 *Phys. Rev.* A **134** 970
[5] Durham P J, Pendry J B and Hodges C H 1982 *Comput. Phys. Commun.* **25** 193
[6] Vvedensky D D, Saldin D K and Pendry J B 1986 *Comput. Phys. Commun.* **40** 421
[7] Herman F and Skillman S 1963 *Atomic Structure Calculations* (Englewood Cliffs, NJ: Prentice-Hall)
[8] Schwartz K 1972 *Phys. Rev.* B **5** 2466
[9] Durham P J, Pendy J B and Hodges C H 1981 *Solid State Commun.* **38** 159
[10] Mele E J and Ritsko J J 1979 *Phys. Rev. Lett.* **43** 68
[11] Batson P E 1993 *Phys. Rev.* B **48** 2608
[12] McCulloch D G, Prawer S and Hoffman A 1994 *Phys. Rev.* B **50** 5905
[13] Pickard C J, Payne M C, Brown L M and Gibbs M N 1996 *Inst. Phys. Conf. Ser. 147* (Bristol: Institute of Physics Publishing) p 211
[14] Fischer D A, Wentzcovitch R M and Carr R G 1991 *Phys. Rev.* B **44** 1427